



HHS Public Access

Author manuscript

Biochem Pharmacol. Author manuscript; available in PMC 2017 September 01.

Published in final edited form as:

Biochem Pharmacol. 2016 September 1; 115: 123–133. doi:10.1016/j.bcp.2016.06.011.

An Engineered Heterodimeric Model to Investigate SULT1B1 Dependence on Intersubunit Communication

Zachary E. Tibbs^a and Charles N. Falany^a

Zachary E. Tibbs: ztibbs@uab.edu; Charles N. Falany: cfalany@uab.edu

^aThe Department of Pharmacology and Toxicology, the University of Alabama at Birmingham School of Medicine, Birmingham, Alabama 35294-0019

Abstract

Cytosolic sulfotransferases (SULTs) biotransform small molecules to polar sulfate esters as a means to alter their activities within the body. Understanding the molecular mechanism by which the SULTs perform their function is important for optimizing future therapeutic applications. Recent evidence suggests each SULT isoform acts by a half-site reaction (HSR) mechanism, in which a single SULT dimer subunit is active at any given time. HSR requires communication through the highly conserved KxxxTVxxxE dimerization motif. In this investigation, we sought to test the intersubunit interactions of SULT1B1 as it relates to enzyme activity. We generated two populations of SULT1B1 isoforms that efficiently heterodimerize upon mixing by targeted point mutation of the KxxxTVxxxE motif to KxxxTVxxxK or ExxxTVxxxE. The heterodimer exhibited wildtype-like activity with regards to native size, thermal integrity, PAP affinity, and PAPS K_m , therefore serving as a valid model for investigating SULT1B1 dimer subunit interactions. The approach granted control over each independent subunit, permitting mutation of the critical 3'-phosphoadenosine 5'-phosphosulfate (PAPS) binding residue Arg258 and/or the catalytic base His109 in a single subunit of the dimer. Substitution of the dysfunctional subunits for fully active subunits yielded dimeric SULT1B1 with 50% the activity of the fully competent dimer, suggesting SULT1B1 intersubunit communication does not significantly contribute to the isoform's activity. These results are a testament to the unique properties of individual SULT isoforms. The dimerization system described in this manuscript can be used to study subunit interactions in other SULT isoforms as well as proteins in other families.

Graphical abstract

Address correspondence to: Charles N. Falany, Department of Pharmacology and Toxicology, University of Alabama at Birmingham, Birmingham, AL 35205. cfalany@uab.edu. Telephone: 1-205-934-9848. Fax: 1-205-934-8240.

Conflict of Interest: The authors declare no conflict of interest.

Authorship Contributions

Participated in research design: Tibbs and Falany

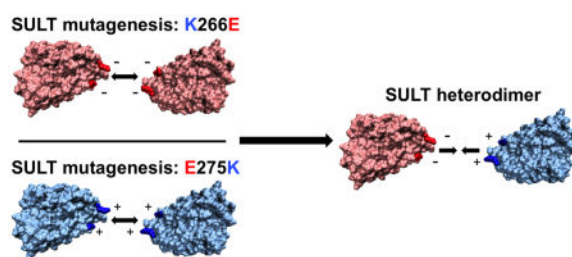
Conducted experiments: Tibbs

Contributed new reagents or analytical tools: Tibbs and Falany

Performed data analysis: Tibbs and Falany

Wrote or contributed to the writing of the manuscript: Tibbs and Falany

Publisher's Disclaimer: This is a PDF file of an unedited manuscript that has been accepted for publication. As a service to our customers we are providing this early version of the manuscript. The manuscript will undergo copyediting, typesetting, and review of the resulting proof before it is published in its final citable form. Please note that during the production process errors may be discovered which could affect the content, and all legal disclaimers that apply to the journal pertain.



Keywords

Drug metabolism; sulfation; protein engineering; half-site reactivity; SULT1B1

1. Introduction

Organisms regulate hormone and small molecule activities by a number of biotransformation pathways, one of which is sulfonate conjugation. Compared to a hydrophobic compound, its sulfate ester is generally more water-soluble, has an altered affinity for receptors, and can be actively exported out of the cell and eventually the body [1–3]. The cytosolic sulfotransferases (SULTs) are responsible for sulfo-conjugation of small molecules in the body, catalyzing the transfer of a sulfonate group from the ATP-like cofactor, 3'-phosphoadenosine 5'-phosphosulfate (PAPS), to the recipient compound [4, 5]. Individual SULT isoforms have unique substrate specificity patterns but share a conserved reaction mechanism, reflected by their conserved architecture [6–8]. Aside from the catalytic residues in the SULT's pore, the most highly conserved region of the SULT includes the dimerization and PAPS binding domains, found directly adjacent to one another (Figure 1) [6, 9, 10]. Each isoform must bind PAPS to perform its function therefore providing an understandable rationale for the conservation of PAPS-interacting amino acids. No discernable role has been identified for SULT dimerization; therefore its conservation remains unwarranted.

Since its identification in 2000, the abnormally small physiological dimerization motif (KxxxTVxxxE) of SULTs has been the subject of multiple investigations [9] (Figure 1). Lu et. al reported no activity differences between a point-mutant monomeric isoform of hSULT1A1 and the wild-type dimer [11]. The group did, however, show the monomeric isoform was susceptible to thermal degradation and therefore determined the dimerization of hSULT1A1 played a role in enzyme integrity [11]. Another study reported loss of substrate inhibition upon monomerization of hSULT2A1, suggesting a link between SULT dimerization and substrate selectivity [12]. Though not directly targeted toward SULT dimerization, recent investigations insinuate a mechanistic role for SULT dimerization in at least three SULT isoforms; hSULT1A1, hSULT2A1, and hSULT1E1 [13–15]. These three isoforms have been reported as acting via a half-site reaction mechanism, a mechanism in which only half of the subunits catalyze the sulfonation reaction at any given time.

Half-site reaction mechanisms require intersubunit communication and often result in an entity with greater catalytic efficiency than the additive activities of the individual subunits

[16]. Recent evidence suggests the binding of cofactor (PAPS) to the SULT induces structural asymmetry that drives communication between dimeric SULT subunits, contributing to SULT half-site reactivity. [17]. The aim of this investigation is to test the capacity of cofactor binding and catalysis to drive such intersubunit communication *in vitro* by engineering a SULT1B1 dimer with interchangeable functional and dysfunctional subunits.

2. Materials and Methods

2.1 Approach

This study necessitated the complete control of SULT1B1 dimerization or the direct comparison of monomeric and dimeric isoforms. Based on previous experiments, the on-rate of SULT dimerization greatly outweighs the off-rate therefore complicating isolation of a wildtype monomeric species. Competition driven monomerization of hSULT1B1 by use of a peptide mimetic of the dimerization domain was unsuccessful (unpublished results) therefore we sought to monomerize hSULT1B1 by mutagenesis. The composition of the native dimerization domain of SULTs (KxxxTVxxxE) allowed for the design of a versatile system for control of SULT dimerization. Specifically, mutation of the complementary salt-bridging residues K266 and E275 to an E and a K, respectively, would theoretically result in two enzyme populations with either a predominantly negatively or positively charged dimerization domain. In theory, the independent populations would monomerize by repulsive forces (Figure 2). Attractive forces could then be used to prompt heterodimerization upon mixing, forming a dimer with a scaffold resembling that of native hSULT1B1 (Figure 2). Using this method, the effects of single subunit alterations can be tested, and the dependence of SULT1B1 activity on intersubunit communication probed more in depth.

2.2 Reagents and Chemicals

All restriction enzymes and the Quick Ligase were purchased from New England Biolabs (NEB). The ZR Plasmid Miniprep Classic kit was purchased from ZYMO Research. The GeneJET Gel Extraction Kit, Phusion High-Fidelity DNA Polymerase, and Ni-NTA resin were purchased from Thermo Scientific. PCR primers, mono/dibasic sodium phosphate, glycerol, chloroform, 2-mercaptoethanol, sodium chloride (NaCl), acrylamide, and Isopropyl β -D-1-thiogalactopyranoside (IPTG) were ordered from Fisher Scientific. Agarose was purchased from Denville. Ampicillin, N, N, N', N' - Tetramethylethylenediamine (TEMED), Chloramphenicol, LB Lennox Broth, and 1-naphthol were purchased from Acros Organics. Life Technologies provided the pPROEx HTa plasmid and dNTPs. PAPS was purchased from PerkinElmer. PAP, imidazole, and Sephadex-G100 resin were purchased from Sigma-Aldrich. Gel-filtration standards were purchased from Bio-Rad. Access to an AKTA-FPLC and the 1000mm \times 26mm GE-Healthcare column were generously provided by Dr. Mahmoud el Kouni. Lastly, BL21-DE3-RIL competent *E. coli* were a gift from Dr. Robert C.A.M. van Waardenburg.

2.3 Cloning of Wildtype hSULT1B1

The human SULT1B1 cDNA was isolated from human liver samples and subcloned into the pKK233-2 vector as previously described [18]. PCR was performed to amplify the hSULT1B1 cDNA insert using Phusion High-Fidelity DNA Polymerase and primer pair 1 (Table 1) according to the manufacturer's protocol. After agarose-gel electrophoresis of the PCR product and subsequent extraction of the amplicon from the agarose gel, the insert was subjected to a 1 hr digestion with HindIII-HF restriction enzyme while the pPROEx HTa plasmid was digested with HindIII-HF and Sfo-I. Both the linearized plasmid and digested hSULT1B1 insert were purified by agarose-gel electrophoresis, extracted from the gel, and incubated together with Quick-Ligase for 15 minutes before a small amount of the sample was added to BL21-DE3-RIL competent *E. coli* for transformation. Manufacturer instructions were followed for the remainder of the transformation procedure. The *E. coli* were plated on ampicillin-(100 µg/mL)/chloramphenicol-(50 µg/mL) (Amp⁺/Chlo⁺) LB-agar plates and allowed to incubate overnight at 37°C. After incubation, colonies were selected and cultured to an acceptable density in small volume Amp⁺/Chlo⁺ LB cultures. Plasmids were isolated from these cultures and sequenced by the UAB-Heflin Core Center for Genomic Science using M13rev and pBAD primers. After sequence verification, the high-density *E. coli* cultures were frozen in 50% glycerol at -80°C.

2.4 hSULT1B1 Mutagenesis

The pPROEx HTa-hSULT1B1 plasmid was used as the template for Agilent QuickChange II Site-Directed Mutagenesis in PCR reactions using primer pairs 2, 3, and 4 (Table 1), allowing an extension time of seven minutes for the PFU Ultra II. All contents of the PCR reaction were treated with DpnI restriction endonuclease for 1.5 hours to fragment the template plasmid. After confirmation of their sequences, both SULT1B1-K266E and SULT1B1-E275K plasmids were subsequently the subjects of site-directed mutagenesis with primer pairs 5 and 6, mutating Arg258 to a Lys and His109 to a Tyr (Table 1). All products were transformed into BL21-DE3-RIL competent *E. coli* as described in section 2.3, sequenced, and frozen as glycerol stocks at -80°C.

2.5 Protein Expression and Purification

Small-volume LB (Amp⁺/Chlo⁺) *E. coli* overnight-cultures (from glycerol stocks) were used as starter cultures for 500 mL LB (Amp⁺/Chlo⁺) cultures in 1L Erlenmeyer flasks. The large cultures were allowed to grow at 37°C, shaking 225 rpm, to an optical density (OD₆₀₀) of 0.5 before reducing the temperature to 20°C and inducing hSULT1B1 protein expression with 0.5 mM IPTG. After 4 hours, the cultures were centrifuged for 15 minutes at 10,000 rpm, the supernatant was disposed, and the pelleted bacteria were frozen overnight at -20°C. The following morning, the pellets were thawed on ice and suspended in buffer containing 10 mM sodium phosphate pH 8.0, 10% glycerol, 300 mM NaCl, 10 mM imidazole, and 10 mM 2-mercaptoethanol (Lysis buffer). The bacteria were lysed on ice via sonication immediately after addition of 0.1 mM of phenylmethanesulfonylfluoride (PMSF) for protease inhibition. The sonicate was centrifuged for 15 minutes at 10,000 × g, the pellet was discarded, and the supernatant was applied to a buffer-equilibrated Ni-NTA column (bed-volume 1.5 mL). The column was subsequently rinsed with 25 bed-volumes of Lysis

buffer and eluted with a 10 to 250 mM imidazole gradient. The eluate was collected in fractions and assayed for purity via SDS-polyacrylamide gel electrophoresis, after which pure hSULT1B1 fractions were combined and dialyzed (7 kDa MWCO tubing) twice against one liter of imidazole-lacking Lysis buffer for 5 hours and 16 hours, respectively, at 4°C. The protein preparation was aliquoted and frozen at -80°C for further analyses. This protein expression/purification protocol was conducted for each hSULT1B1 isoform.

2.6 Gel Filtration Chromatography

A 1000mm × 26mm GE-Healthcare chromatography column was packed with Sephadex G-100 resin for size-exclusion chromatography on a Pharmacia AKTA-FPLC. The column was equilibrated at a constant flow of 0.1 mL/min with Lysis buffer lacking imidazole and glycerol, as glycerol's viscosity contributes to unwanted backpressure. Gel filtration standards (Bio-Rad) were injected over the column and elution fractions were collected and assayed for protein content using Bio-Rad Protein Assay reagent. A log transformed standard curve equating size to elution time/volume was constructed from the standards. In separate instances, two milligrams of each hSULT1B1 isoform was injected over the column and assayed for protein content and 1-naphthol sulfation activity. The standard curve was applied to back-calculate the native molecular weight of each hSULT1B1 sample based on its peak elution volume.

2.7 Native Polyacrylamide Gel Electrophoresis (Native-PAGE)

Native-PAGE was performed as a relatively quick and high-throughput assay for determining heterodimerization efficiency. Complete heterodimerization was achieved by co-incubating normalized concentrations of the hSULT1B1-K266E and -E275K isoforms for 1 hour (on ice), therefore this incubation condition was used in each instance prior to any assay. Native-PAGE was performed for 3.5 hours on a bed of ice with a constant power input of 160 V. The gel's separating layer contained 1.5 M Tris (pH 8.8) while the stacking layer contained 0.5 M Tris (pH 6.8). Both layers contained ammonium persulfate and TEMED for polymerization. The separating layer contained 13% acrylamide while the stacking layer contained 4.2% acrylamide. The running buffer contained 25 mM Tris and 192 mM glycine, resulting in a final pH of 8.3. Native gels were visualized with Coomassie Brilliant Blue.

2.8 Enzyme Kinetics Assays

To test the sulfation activity of each SULT isoform, a well-described sulfation assay was employed using ³H-labeled 1-naphthol (American Radiolabeled Chemicals) as the tracer substrate [19]. In the assay, 50 mM Tris (pH 7.4), 5 mM MgCl₂, and select concentrations of PAPS and 1-naphthol were pre-mixed and incubated at 37°C for two minutes, at which point the reaction was initiated by addition of enzyme, vortexed rapidly, and placed back into a 37°C water bath for reaction progression. The reaction was quenched with chloroform (25× reaction volume) and the pH of the quenched reaction was raised by addition of 1.5 M Tris pH 8.8. The reaction tubes were centrifuged for 5 minutes at 1500 rpm and the ³H content in the aqueous layer was quantified via liquid scintillation. The data were analyzed using VisualEnzymics and Igor Pro employing a rapid equilibrium two substrate: random bi bi with substrate inhibition model.

2.9 Thermal Stability Assay

The thermal integrity of the SULT1B1-WT, -E275K, -K266E, and the heterodimeric isoform were evaluated by testing the retention of sulfation activity after incubation of each isoform at either 37°C or 45°C. Thermal incubation of each isoform was quenched by placing the enzyme directly on ice at a series of time points (1, 2, 5, 10, 20, 30, 45, 60, 90 min). After all samples were collected, the activity of each was tested using the enzyme kinetics assay described above (15 μ M PAPS, 10 μ M 1-naphthol). Each isoform's thermal integrity was tested in triplicate. The specific activities measured at each time point were normalized to the specific activity of each isoform prior to thermal incubation.

2.10 Binding Assays

SULT1B1 aromatic residue intrinsic fluorescence (IF) (excitation 282, emission 338) was monitored using a Horiba FluoroMax-4 as a means for evaluating the binding of the cofactor to each isoform. For each SULT1B1 isoform, 0.20 μ M hSULT1B1 was added to buffer (2 mL total volume) (10 mM sodium phosphate pH 7.8, 10% glycerol, 150 mM NaCl) in a quartz cuvette. The desired drug concentration was pipetted into the cuvette (2 μ L increments) while stirring with a spectral cell stir bar. Following a 15 s mixing period, the emission intensity was monitored for 15 s in 0.1 s increments. Each data point was considered to be the average of all 150 IF measurements at the particular drug concentration. This process was continued until the final desired drug concentration was reached. Inner filter effects were observed at high PAP(S) concentrations. To negate the inner filter effects, equimolar concentrations of adenosine monophosphate (AMP), which SULTs do not bind, was titrated into the SULT1B1 solution [20]. This data was then subtracted from the PAP/PAPS binding data as has been described previously [14]. The data were analyzed in VisualEnzymics and Igor Pro assuming a one site binding:simple hyperbolic model.

3. Results

Cloning and purification of each SULT1B1 variant isoform was successful, achieving greater than 90% pure SULT1B1 in each instance (data not shown). Post-freeze (-80°C) specific activity retention was consistently high (95–100%) for each variant isoform. Each isoform was applied to a G100 gel filtration chromatography column to determine its native size. The post-void elution volumes of the K266E, E275K, K266E/E275K heterodimer, and wildtype SULT1B1 isoforms were 30 mL, 21 mL, 16 mL, and 16 mL, respectively (Figure 3A). Based on the standard curve, the calculated molecular weight (MW) of the K266E isoform was 38 kDa (2% different from the expected MW of a SULT1B1 monomer), while the E275K isoform had a calculated MW of 60 kDa (20% different from the expected MW of a SULT1B1 dimer). The rationale for this difference in apparent MW will be entertained in the discussion. The calculated molecular weight of both the wildtype and heterodimeric isoforms was 77 kDa, 2% larger than the expected molecular weight (76 kDa) of a 6xHis-tagged SULT1B1 dimer. To ensure these observed peaks were not the product of enzyme isoform specific activity differences, the protein content of each fraction was also tested using a colorimetric assay (data not shown). The percent sulfation activity shown in Figure 3A was directly correlated with protein concentrations in the fractions. Heterodimerization was further confirmed by native-PAGE (Figure 3B). The K266E isoform clearly migrated

further into the gel, much like the migration pattern of the known monomer, SULT1B1-K266A. Mixing the K266E isoform with the E275K isoform abolished the monomeric species and formed a dimeric complex which migrated similar to wildtype SULT1B1 (Figure 3A and Figure 3B). Small amounts of residual monomer were left behind, though the coupling efficiency was determined to be >95%.

Monomerization has been shown to decrease the thermal stability of hSULT1A1, therefore the thermal stability of each hSULT1B1 isoform was tested at 37°C and 45°C [11]. The wildtype enzyme was stable at both temperatures for at least 90 minutes, showing minimal activity loss after 45°C incubation (Figure 4A). The K266E mutant lost almost all activity after a 90 minute 45°C incubation, while the E275K mutant lost only 30% of its sulfation activity (Figure 4A). The K266E/E275K heterodimeric species resembled that of wildtype SULT1B1, retaining most of its activity after 37°C and 45°C incubation for 90 minutes (Figure 4A).

Both mutations (E275K and K266E) were near the cofactor-binding domain, therefore their abilities to bind the cofactor, PAP(S), were measured. The wildtype enzyme exhibited a PAP K_d of 0.11 μM (Figure 4B). The K266E monomer suffered a detriment to its affinity for PAP, measuring 1.47 μM , while the E275K mutant had a more favorable K_d (0.08 μM) than wildtype SULT1B1 (Figure 4B). The heterodimeric species' K_d for PAP was similar to that of wildtype SULT1B1, 0.18 μM (Figure 4B). The affinities of each isoform for the cofactor were reflected in the PAPS K_m 's, where the WT and heterodimeric SULT1B1 isoforms exhibited K_m 's of 1.97 and 1.90 μM , respectively (Figure 4C). The K266E isoform displayed a diminished PAPS K_m (3.88 μM), while the E275K isoform's PAPS K_m (1.58 μM) was similar to WT, trending toward a more favorable value.

The purpose of generating a heterodimeric SULT1B1 species that replicated wildtype activity was to allow independent control of each individual subunit as a means for testing the contribution of intersubunit communication to enzyme activity. Therefore, we targeted both subunits with mutations which disabled the ability of the subunit to (1) bind PAPS and undergo concerted structural shifts upon its binding, (2) catalyze sulfuryl transfer, or (3) both. Each mutant isoform was successfully purified and confirmed to retain its heterodimerization properties via native-PAGE (Figure 5A). The R258K and H109Y mutations minimally affected the native-gel migration pattern of each independent isoform. After mixing each mutant with heterodimeric partners, nearly all of the monomer-sized bands were abolished. For further validation, gel filtration was used to confirm the SULT1B1-K266E isoform heterodimerized with each potential partner (Figure 5B).

After confirmation of efficient heterodimerization, the activity properties were tested. The ability of each isoform to bind the cofactor was first confirmed. The dissociation constants of each monomeric and heterodimeric isoform are summarized in Table 2. Briefly, mutation of R258K, regardless of other mutations, rendered the isoform unable to bind PAP at detectable levels up to 12 μM while the H109Y mutation negatively affected PAP binding by approximately 10-fold. Binding curves for each E275K isoform by itself and heterodimerized with the K266E subunit are shown in Figure 6. The K_d 's in Table 2 do not fully encompass the information provided by the binding curves, as they do not describe the

magnitude of IF change observed. The IF decreased nearly 14% before saturated binding was achieved for the K266E isoform, alone, and when it was coupled with the E275K subunit. When the K266E isoform was coupled with the R258K and H109Y mutant subunits, the IF only decreased by nearly 7%, suggesting half-site binding.

The specific activity of each independent and heterodimeric isoform toward 1-naphthol were measured (Figure 7). The K266E/E275K heterodimer was the most active isoform (0.203 pmol/($\mu\text{g}\cdot\text{s}$)), displaying greater activity than the independent K266E and E275K isoforms. In every case, mutation of H109Y completely abolished activity (Figure 7). No activity was detected when R258 was mutated to K in the K266E background, while nearly 10% activity was retained when R258 was mutated to a K in the E275K background. When the H109Y, R258K, and R258K-H109Y subunits were coupled with fully competent subunits (i.e. K266E or E275K), the specific activities proved to be additive. For the purpose of comparison, each specific activity was normalized to the K266E/E275K heterodimer's specific activity. To compare the activities in Figure 7, one must be aware that the activities were first normalized for protein concentration. For example, to compare the independent activities of the K266E and E275K isoforms to the K266E/E275K heterodimer: Independently, the K266E and E275K isoforms displayed 62% and 92% the specific activity of the K266E/E275K heterodimer, respectively. The additive value (154%) is not comparable to the K266E/E275K's heterodimer's 100% value. Instead, 154% must be divided in half to account for the doubled protein concentration. Therefore, the K266E/E275K heterodimer is 130% (77%/100%) more efficient than the independent subunit activities.

4. Discussion

Testing the dependence of SULT1B1 activity on the communication between its dimeric subunits required control of subunit coupling. To avoid the potential detrimental effects of mutation itself, we first attempted to compete SULT1B1 subunits apart with a peptide mimetic of the dimerization domain ($^+\text{NH}_3\text{-WKNYFTVAQNEK-COO}^-$). Heated co-incubation of the peptide and pure wildtype SULT1B1 enzyme yielded no monomeric enzyme for activity comparisons. Further, the dependence of wildtype SULT1B1 and SULT1B1-K266L (monomeric) dimerization was tested in both the presence and absence of a saturating concentration (70 μM) of PAP. PAP had no effect on the dimerization status of either SULT1B1 isoform, as is supported in each SULT crystal structure (with our without the cofactor) resolved to date [21, 22]. These anecdotal observations of the subunit coupling affinity could provide a rationale for the lack of historical reports of the existence of physiological SULT heterodimers, despite conservation of identical dimerization domains across isoforms (Figure 1) [23, 24]. SULTs may irreversibly dimerize directly off of the ribosome following translation.

To overcome the limitation in generating monomeric SULT1B1 for study, we initially relied on the mutation of the conserved dimerization residue, K266, to an Ala and a Leu (abolishing electrostatic potential). The K266A and K266L isoforms were monomeric and exhibited altered activities with regards to their interactions with the cofactor, PAPS. Concern was raised that altered activity was due to the mutated residue itself and not

necessarily the lack of dimerization. Therefore, we designed a more versatile system to allow control of each SULT1B1 subunit independently, making use of the native electrostatic properties of the SULT's KxxxTVxxxE dimerization domain. SULT point mutants, consisting of the dimerization domain sequences KxxxTVxxxK and ExxxTVxxxE, would theoretically heterodimerize upon mixing due to attractive forces. This wildtype-like heterodimer was then used as a control isoform while each subunit was independently substituted with dysfunctional subunits to probe the contribution of intersubunit interactions to SULT1B1 activity.

Mutation of K266 and E275 to the reciprocally charged residues abrogated salt-bridging ability but did not appear to monomerize SULT1B1 in each instance. Mutation of K266 to an E rendered the enzyme monomeric while the native MW of the E275K mutant most closely resembled a dimer. The interfacing surface area of SULT subunits is very small, giving the SULT dimer a dumbbell-like architecture. The E275K mutation may have collapsed the dimerization domain causing the interfacing surface area to be larger, in turn producing an apparent reduction in the MW of the isoform (60 kDa instead of 76 kDa). This hypothesis requires further investigation for validation. Regardless, the non-reciprocal result of mutation of the pairing residues suggests SULT dimerization does not require the salt-bridge between Lys266 and Glu275. Conservation of secondary structure may actually play the largest role in mediating SULT dimerization (Figure 8). K266 is located in the middle of a single turn helix, an important, yet somewhat unstable, structure for maintaining correct orientation of the critical β -bridging Phe and Val dimerization residues (Figure 8) [9]. Mutation of K266 may destabilize this secondary structure, abolishing SULT dimerization. E275 is located in the middle of a five-turn helix, therefore its mutation may not be detrimental to maintenance of secondary structure, thus not dimerization. The monomeric isoform was thermo-labile, consistent with this hypothesis and previous literature regarding monomeric SULT1A1; further strengthening the notion that SULT dimerization is important for subunit stability in the cell [11]. Though this study lacks evidence for an alternative explanation for the conservation of SULT dimerization, other reports indicate the domain contributes to the enzymatic mechanism, and not only structural integrity [13, 14].

While the enzyme populations did not behave as expected independently, they readily heterodimerized as predicted following a 1 hour 1:1 (mol:mol) incubation at 4°C, suggesting the abnormal interaction along the E275K homodimer was relatively unstable. The results in this study were dependent on the formation of the expected protein species; therefore any level of confirmation of the K266E/E275K species was beneficial in our interpretation of the results. Activity studies heavily supported the notion that the heterodimer was efficiently formed. Both the K266E and E275K isoforms exhibited abnormal activities with regard to their PAP dissociation and Michaelis-Menten constants (Figure 4B–C). These detriments, as well as overall size and thermal-integrity were rescued by heterodimerization (Figure 3 and Figure 4). Based on this evidence, the K266E/E275K heterodimeric species was determined to be a good model for further investigation of the subunit interdependence of the SULT1B1 dimer as it relates to activity.

Residues critical for SULT function were mutated to probe the dependence of each subunit on its dimer partner's activity. Arg258 is critical for mediating structural shift of the SULT

backbone upon PAPS binding via its direct interaction with the cofactor's 3' phosphate group [21, 25, 26]. Arg258 is thought to "sense" the orientation of PAP(S) within the active site of the enzyme, possibly allowing communication to the partnering subunit [17]. Mutation of Arg258 to a Lys was confirmed to heavily diminish PAPS binding by SULT1B1 prior to its use in the heterodimer system (data not shown). The catalytic base histidine (His109) was also substituted to a Tyr to abolish its catalytic base potential. Mutation of His109 to Ser, Leu, and Arg abolishes SULT activity, while mutation to a Lys yields an isoform with 100 fold less activity which is gradually lost over time [27]. The loss of enzyme activity over time in Kakuta's study prompted our desire to conserve the residue's aromaticity, for the sake of enzyme stability, while still abolishing its catalytic base activity.

The R258K and H109Y mutations were performed in both K266E and E275K mutant backgrounds and the resulting isoforms were confirmed to heterodimerize via native-PAGE. Small amounts of the monomeric isoform (K266E background) were still present after co-incubation with the E275K isoforms, though heterodimerization was efficient (>95%). Some isoforms showed greater heterodimerization efficiency than others. The result may represent the true dimerization efficiencies of point-mutant isoforms, though only R258K is in position to potentially interfere with dimerization. Based on the native-PAGE banding patterns, we favor the hypothesis that this result was due to unnormalized protein concentrations, despite our best efforts for normalization. Inevitably, the low level of unwanted monomeric isoforms contributed to activity (catalysis and binding) measurements, though their contribution had a minimal effect on each value.

The activities of each individual isoform and isoform combination were then tested to (1) ensure the R258K mutation diminished PAP(S) binding (2) confirm the H109Y mutation abolished catalytic activity (3) and test for synergistic subunit interactions. In general, the R258K mutation abolished the ability of SULT1B1 to bind PAP. Substitution of the E275K subunit with the E275K-R258K subunit diminished the PAP K_d slightly (0.33 μM), suggesting Arg258 activity in the neighboring subunit may contribute, in some manner, to PAP binding affinity in its partner. The saturation point of binding in the K266E/E275K-R258K heterodimer was achieved at 8% change in IF, half that of the K266E/E275K heterodimer (~16%), implying PAP bound to a single side of the dimer, as expected (Figure 6). In addition to the R258K mutation abolishing PAP binding, mutation of His109 to a Tyr caused a 10-fold decrease in PAP binding affinity (0.67 μM) compared to the control isoform (E275K). Oddly, the H109Y mutation in a single subunit of the dimer also resulted in a dimer that approached saturated binding at 8% change, suggesting the presence of a Tyr in place of the active site His rendered the subunit unable to bind PAP when coupled with a PAP-bound subunit. While attempting to maintain structural density and aromaticity at the 109th amino acid position, overall size conservation of the residue was sacrificed. In the H109Y isoform, the tyrosine likely protrudes into the binding pocket of SULT1B1 and sterically interferes with PAP binding, resulting in an overall lower binding affinity. Though the results are not documented in this study, mutation of His109 to a Phe also inhibited the ability of SULT1B1 to bind PAP, suggesting substitution of His109 with a smaller amino acid may be the best way to retain potent PAP affinity while abolishing catalytic activity.

Each heterodimer's specific activity toward 1-naphthol was measured as an indicator of catalysis (Figure 7). To our knowledge, no one has described the effect of Arg258 mutation, whereas the effect of His109 mutation on SULT catalysis has been discussed prior to this report. Mutation of His109 to a Tyr completely abolished sulfation activity in each case, regardless of other mutations, due to tyrosine's inability to act as a catalytic base. Mutation of Arg258 to a Lys essentially rendered the enzyme inactive, with a low level of residual activity in the E275K-R258K isoform. Based on the specific activities, the K266E/E275K heterodimeric subunits first appeared to display synergistic gain in specific activity once they were coupled together. This synergy was tested by measuring the activity of a fully competent subunit (e.g. K266E) paired with the dysfunctional subunits. Compared to the heterodimer with two competent subunits, the K266E/E275K-R258K and K266E-R258K/E275K heterodimer activities most closely resembled additive activities, not synergistic activities, with 50% the activity of the fully active dimer (Figure 7). Coupled with the observation that the K266E/E275K-H109Y and K266E-H109Y/E275K heterodimers display approximately 50% of the activity of the K266E/E275K heterodimer, we determined the data does not support a SULT1B1 catalytic mechanism that is heavily reliant on coordinated intersubunit communication; one dependent on oscillating binding/catalysis.

In this investigation, we showed dimerization significantly contributes to the thermal stability of SULT1B1, consistent with other isoforms [11]. We further established the contribution of three conserved amino acids (Arg258, Lys266, and Glu275) to SULT oligomerization and catalytic activity, while reinforcing the role of a fourth well-described residue (His109) [27]. Pre-steady state kinetics have been used to describe other SULTs (SULT1E1, SULT1A1, and SULT2A1) as half-site reactive isoforms [13–15]. Despite our best efforts to resolve a pre-steady state sulfation phase for SULT1B1, no such “burst” phase has been detected with any substrate, thus complicating determination of its half-site or full-site mechanism. Therefore, a versatile system for creating SULT1B1 heterodimers was developed to test the dependence of SULT1B1 activity on the communication between its dimeric subunits. Using this system, we detected no such intersubunit dependence for maintenance of activity; providing no evidence to suggest SULT1B1 is a half-site reactive isoform. This conclusion could be strengthened by testing the heterodimerization system in a second SULT, one that relies on intersubunit communication.

Using another SULT, intricacies of the interdependence of subunit activities could be investigated in greater depth. It is unlikely that intersubunit communication is independent of both PAPS binding and catalysis, therefore was assumed throughout this study. This could be explicitly shown using another SULT isoform. The current study was limited by the substitution of Lys266 and Glu275 with amino acids bearing shorter and longer R-group lengths, respectively. While unlikely, the length difference could disrupt coordination between dimer subunits. Another SULT could be used to test the substitution of Lys266 and Glu275 with unnatural amino acids; amino acids with the conserved R-group length in combination with the charges used in this study. These substitutions would result in a SULT heterodimer that resembles the native SULT even more closely than the one in our report, and may actually yield greater dimerization efficiency than that observed in this study.

The rewards from this study are two-fold. First, we have gained an appreciation for SULT isoform uniqueness by showing SULT1B1's activity is not heavily dependent on intersubunit communication, like others in the enzyme family. Otherwise, abolishing the cofactor-binding and/or catalytic competency of a single subunit of SULT1B1 would have altered the activity of the pairing subunit. Second, we have described a system for controlling subunit dimerization that can be used to investigate the intersubunit dependence of other oligomeric metabolic enzyme families. After all, the more we understand about the biochemical mechanisms underlying drug-metabolizing enzyme functions, the more readily we can alter their activities in ways that benefit modern medicine.

Acknowledgments

The authors thank Dr. Mahmoud el Kouni, Dr. Robert C.A.M. van Waardenburg, and Dr. Steve Aller for their generous donations of reagents, equipment, and ideas that contributed to this project.

Funding: This work was supported by the National Institutes of Health Grant GM38953 to CNF.

Abbreviations

PAP	3',5'-diphosphoadenosine
PAPS	3'-phosphoadenosine 5'-phosphosulfate
SULT	cytosolic sulfotransferase

References

1. Strott CA. Sulfonation and molecular action. *Endocrine reviews*. 2002; 23:703–32. [PubMed: 12372849]
2. Kotov A, Falany JL, Wang J, Falany CN. Regulation of estrogen activity by sulfation in human Ishikawa endometrial adenocarcinoma cells. *The Journal of steroid biochemistry and molecular biology*. 1999; 68:137–44. [PubMed: 10369411]
3. Cook IT, Duniec-Dmouchowski Z, Kocarek TA, Runge-Morris M, Falany CN. 24-hydroxycholesterol sulfation by human cytosolic sulfotransferases: formation of monosulfates and disulfates, molecular modeling, sulfatase sensitivity, and inhibition of liver x receptor activation. *Drug metabolism and disposition: the biological fate of chemicals*. 2009; 37:2069–78. [PubMed: 19589875]
4. Falany CN. Enzymology of human cytosolic sulfotransferases. *FASEB journal : official publication of the Federation of American Societies for Experimental Biology*. 1997; 11:206–16. [PubMed: 9068609]
5. Suzuki S, Strominger JL. Enzymatic sulfation of mucopolysaccharides in hen oviduct. I. Transfer of sulfate from 3'-phosphoadenosine 5'-phosphosulfate to mucopolysaccharides. *The Journal of biological chemistry*. 1960; 235:257–66. [PubMed: 13835879]
6. Allali-Hassani A, Pan PW, Dombrowski L, Najmanovich R, Tempel W, Dong A, et al. Structural and chemical profiling of the human cytosolic sulfotransferases. *PLoS biology*. 2007; 5:e97. [PubMed: 17425406]
7. Tibbs ZE, Rohn-Glowacki KJ, Crittenden F, Guidry AL, Falany CN. Structural plasticity in the human cytosolic sulfotransferase dimer and its role in substrate selectivity and catalysis. *Drug Metab Pharmacokinet*. 2015; 30:3–20. [PubMed: 25760527]
8. Gamage N, Barnett A, Hempel N, Duggleby RG, Windmill KF, Martin JL, et al. Human sulfotransferases and their role in chemical metabolism. *Toxicological sciences : an official journal of the Society of Toxicology*. 2006; 90:5–22. [PubMed: 16322073]
9. Petrotchenko EV, Pedersen LC, Borchers CH, Tomer KB, Negishi M. The dimerization motif of cytosolic sulfotransferases. *FEBS letters*. 2001; 490:39–43. [PubMed: 11172807]

10. Weitzner B, Meehan T, Xu Q, Dunbrack RL Jr. An unusually small dimer interface is observed in all available crystal structures of cytosolic sulfotransferases. *Proteins*. 2009; 75:289–95. [PubMed: 19173308]
11. Lu LY, Chiang HP, Chen WT, Yang YS. Dimerization is responsible for the structural stability of human sulfotransferase 1A1. *Drug metabolism and disposition: the biological fate of chemicals*. 2009; 37:1083–8. [PubMed: 19237513]
12. Cook IT, Leyh TS, Kadlubar SA, Falany CN. Lack of substrate inhibition in a monomeric form of human cytosolic SULT2A1. *Hormone molecular biology and clinical investigation*. 2010; 3:357–66. [PubMed: 21822453]
13. Sun M, Leyh TS. The human estrogen sulfotransferase: a half-site reactive enzyme. *Biochemistry*. 2010; 49:4779–85. [PubMed: 20429582]
14. Wang T, Cook I, Leyh TS. 3'-Phosphoadenosine 5'-phosphosulfate allosterically regulates sulfotransferase turnover. *Biochemistry*. 2014; 53:6893–900. [PubMed: 25314023]
15. Wang T, Cook I, Falany CN, Leyh TS. Paradigms of Sulfotransferase Catalysis - The Mechanism of SULT2A1. *The Journal of biological chemistry*. 2014
16. Mochalkin I, Miller JR, Evdokimov A, Lightle S, Yan C, Stover CK, et al. Structural evidence for substrate-induced synergism and half-sites reactivity in biotin carboxylase. *Protein science : a publication of the Protein Society*. 2008; 17:1706–18. [PubMed: 18725455]
17. Tibbs ZE, Falany CN. Dimeric human sulfotransferase 1B1 displays cofactor-dependent subunit communication. *Pharmacology research & perspectives*. 2015; 3:e00147. [PubMed: 26236487]
18. Wang J, Falany JL, Falany CN. Expression and characterization of a novel thyroid hormone-sulfating form of cytosolic sulfotransferase from human liver. *Molecular pharmacology*. 1998; 53:274–82. [PubMed: 9463486]
19. Rohn KJ, Cook IT, Leyh TS, Kadlubar SA, Falany CN. Potent inhibition of human sulfotransferase 1A1 by 17alpha-ethinylestradiol: role of 3'-phosphoadenosine 5'-phosphosulfate binding and structural rearrangements in regulating inhibition and activity. *Drug metabolism and disposition: the biological fate of chemicals*. 2012; 40:1588–95. [PubMed: 22593037]
20. Rens-Domiano SS, Roth JA. Inhibition of M and P phenol sulfotransferase by analogues of 3'-phosphoadenosine-5'-phosphosulfate. *Journal of neurochemistry*. 1987; 48:1411–5. [PubMed: 3470439]
21. Rehse PH, Zhou M, Lin SX. Crystal structure of human dehydroepiandrosterone sulphotransferase in complex with substrate. *The Biochemical journal*. 2002; 364:165–71. [PubMed: 11988089]
22. Chang HJ, Shi R, Rehse P, Lin SX. Identifying androsterone (ADT) as a cognate substrate for human dehydroepiandrosterone sulfotransferase (DHEA-ST) important for steroid homeostasis: structure of the enzyme-ADT complex. *The Journal of biological chemistry*. 2004; 279:2689–96. [PubMed: 14573603]
23. Kiehlbauch CC, Lam YF, Ringer DP. Homodimeric and heterodimeric aryl sulfotransferases catalyze the sulfuric acid esterification of N-hydroxy-2-acetylaminofluorene. *The Journal of biological chemistry*. 1995; 270:18941–7. [PubMed: 7642552]
24. Heroux JA, Roth JA. Physical characterization of a monoamine-sulfating form of phenol sulfotransferase from human platelets. *Molecular pharmacology*. 1988; 34:194–9. [PubMed: 3166104]
25. Cook IT, Leyh TS, Kadlubar SA, Falany CN. Structural rearrangement of SULT2A1: effects on dehydroepiandrosterone and raloxifene sulfation. *Hormone molecular biology and clinical investigation*. 2010; 1:81–7. [PubMed: 21822452]
26. Pedersen LC, Petrochenko EV, Negishi M. Crystal structure of SULT2A3, human hydroxysteroid sulfotransferase. *FEBS letters*. 2000; 475:61–4. [PubMed: 10854859]
27. Kakuta Y. The Sulfuryl Transfer Mechanism. Crystal Structure of a Vanadate Complex of Estrogen Sulfotransferase and Mutational Analysis. *Journal of Biological Chemistry*. 1998; 273:27325–30. [PubMed: 9765259]
28. Pan PW, Tempel W, Dong A, Loppnau P, Kozieradzki I, Edwards AM, Arrowsmith CH, Weigelt J, Bountra C, Bochkarev A, Min J. Crystal structure of human cytosolic sulfotransferase SULT1B1 in complex with PAP and resveratrol. 2008

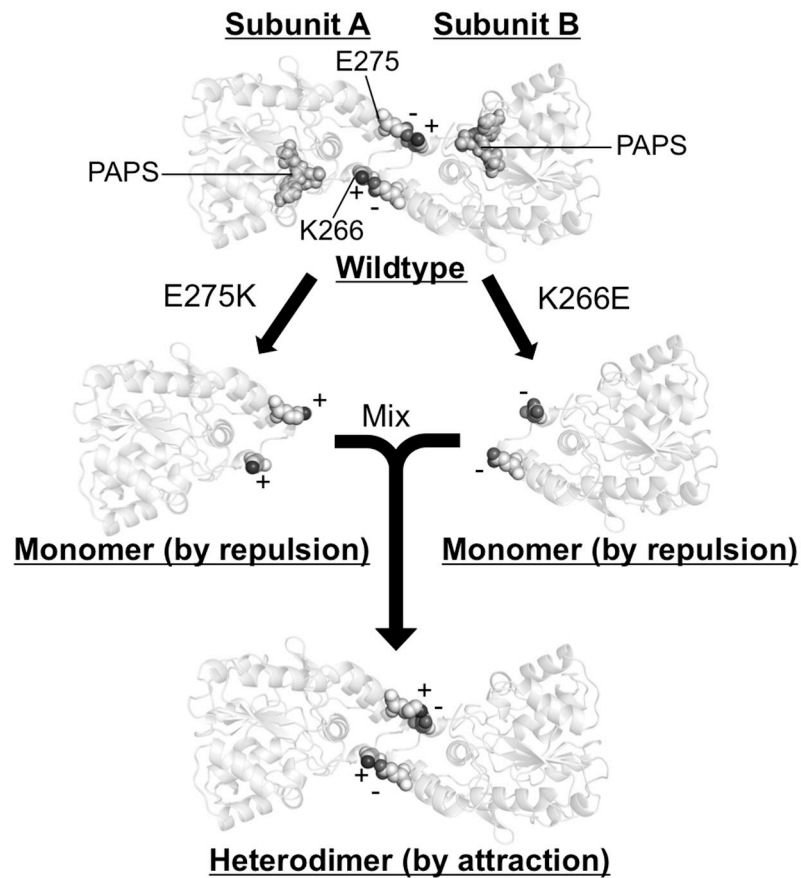


Figure 2. Schematic for controlling SULT1B1 dimerization [28]. SULTs have salt bridging dimerization residues K266 (+) and E275 (-), nearby the PAPS (spheres) binding domain. Mutation of E275 to a K and K266 to an E results in either a dominantly positive or dominantly negative charged dimerization domain, disallowing dimerization via repulsive forces. Mixing of the two populations should yield a heterodimeric complex via attraction.

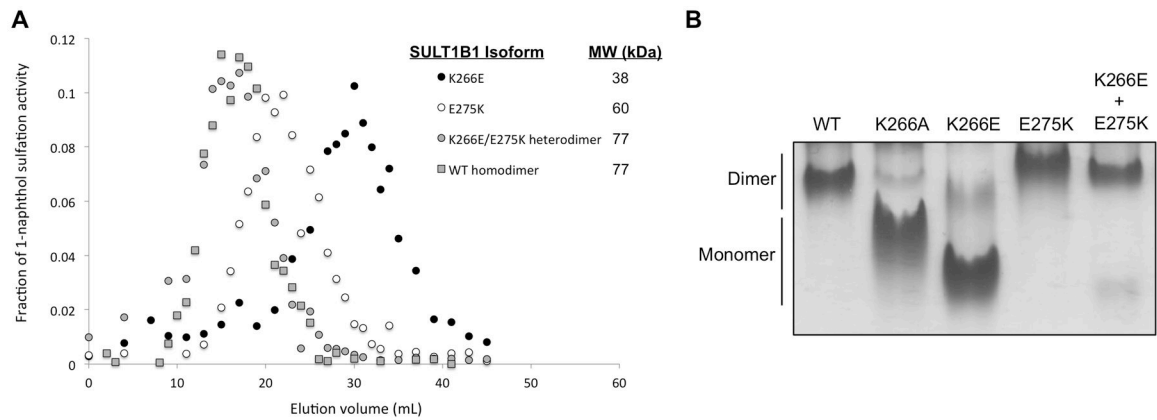


Figure 3.

Confirmation of the SULT1B1 heterodimer formation (A) SULT1B1-K266E (black circle) elutes as a monomer (38 kDa) from a G100 gel filtration column while SULT1B1-E275K (white circle) elutes at an unexpected size of 60 kDa. The reason for the unexpected size is entertained in the discussion. After incubation together, SULT1B1-K266E and E275K co-elute as a 77 kDa dimer (grey circle), the same size as the wildtype dimer (grey square). (B) Native-PAGE shows the SULT1B1-K266E isoform is monomeric, migrating similar to the positive control SULT1B1-K266A isoform. SULT1B1-E275K migrates slightly higher than WT-SULT1B1 (dimer). Mixing the K266E and E275K isoforms together almost completely abolishes the K266E monomer band, forming a species that migrates very similar to WT-SULT1B1. High-resolution native-PAGE results were dependent on retention of the N-terminal 6xHis tag. The 6xHis tag contributes to low-affinity higher order (tetrameric) species upstream of the pictured dimer. Confirmation of these higher order species as artifacts at relevant concentrations was provided by gel filtration.

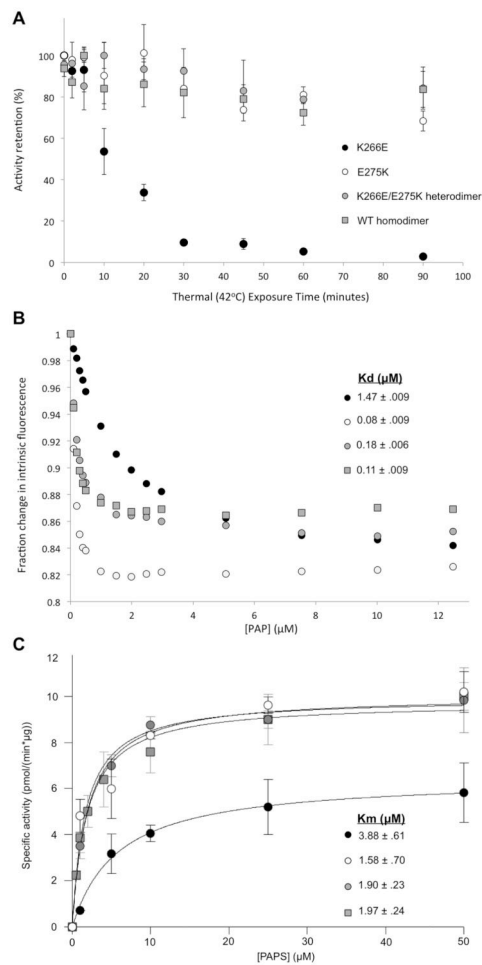


Figure 4. Rescue of SULT1B1-WT-like activities by SULT1B1-K266E/-E275K heterodimerization. (A) Thermal sensitivity, (B) the PAP dissociation constant, and (C) PAPS K_m/V_{max} for each “monomeric” population are rescued by heterodimerization (refer to key). Each data set represents the mean of triplicate experiments with error bars depicting SEM.

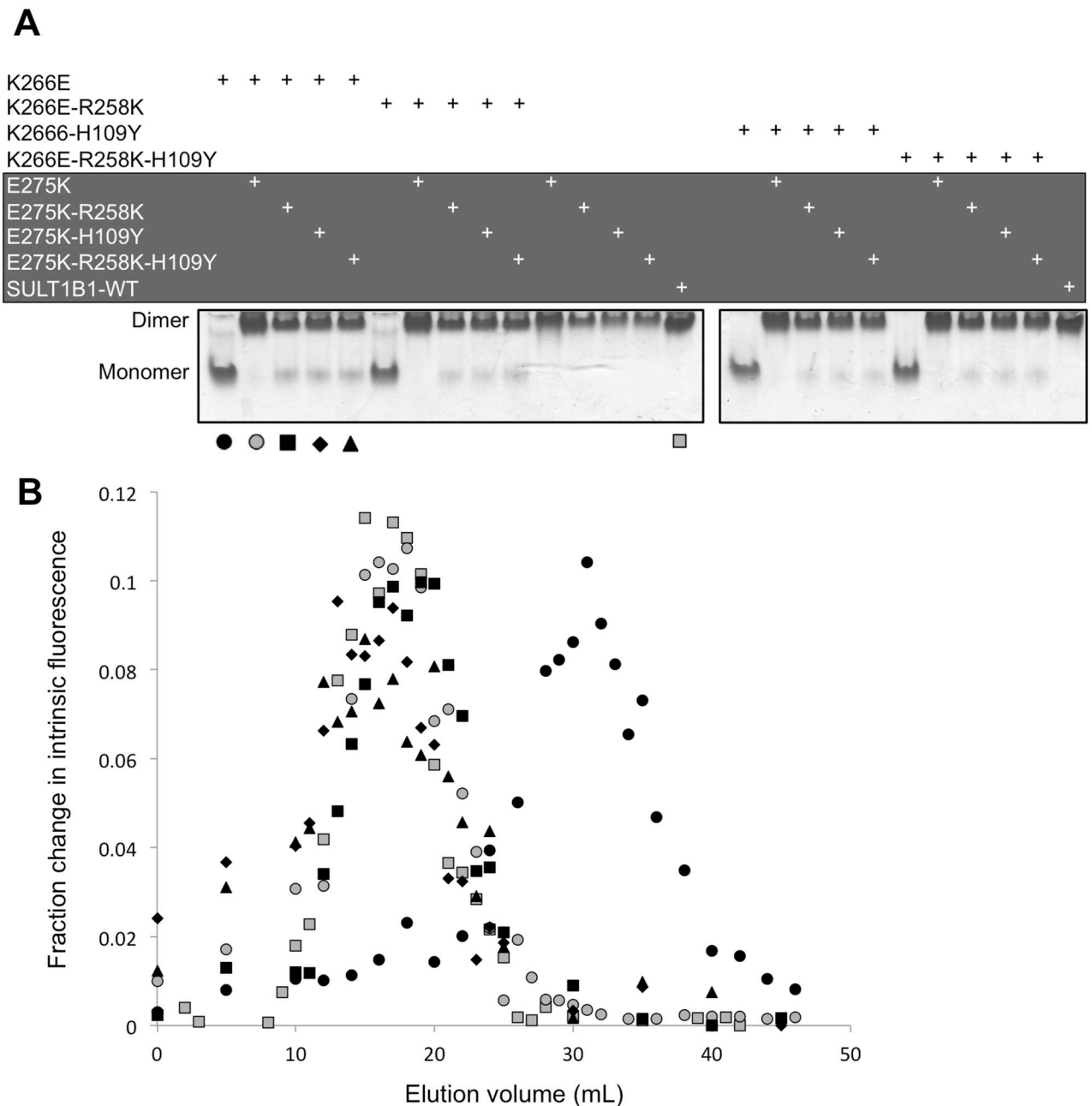


Figure 5.

Heterodimerization between each SULT1B1 subunit. (A) Native-PAGE was used as a high-throughput method to ensure addition of the extra mutations (R258K, H109Y, or both) did not negatively affect heterodimerization between subunits. (B) Gel filtration chromatography confirmed, with higher resolution, the formation of heterodimers between the SULT1B1-K266E subunit (black circle) and E275K (grey circle), E275K-R258K (black square), E275K-H109Y (black diamond), or E275K-R258K-H109Y (black triangle). The heterodimers eluted at the same size as SULT1B1-WT (grey square).

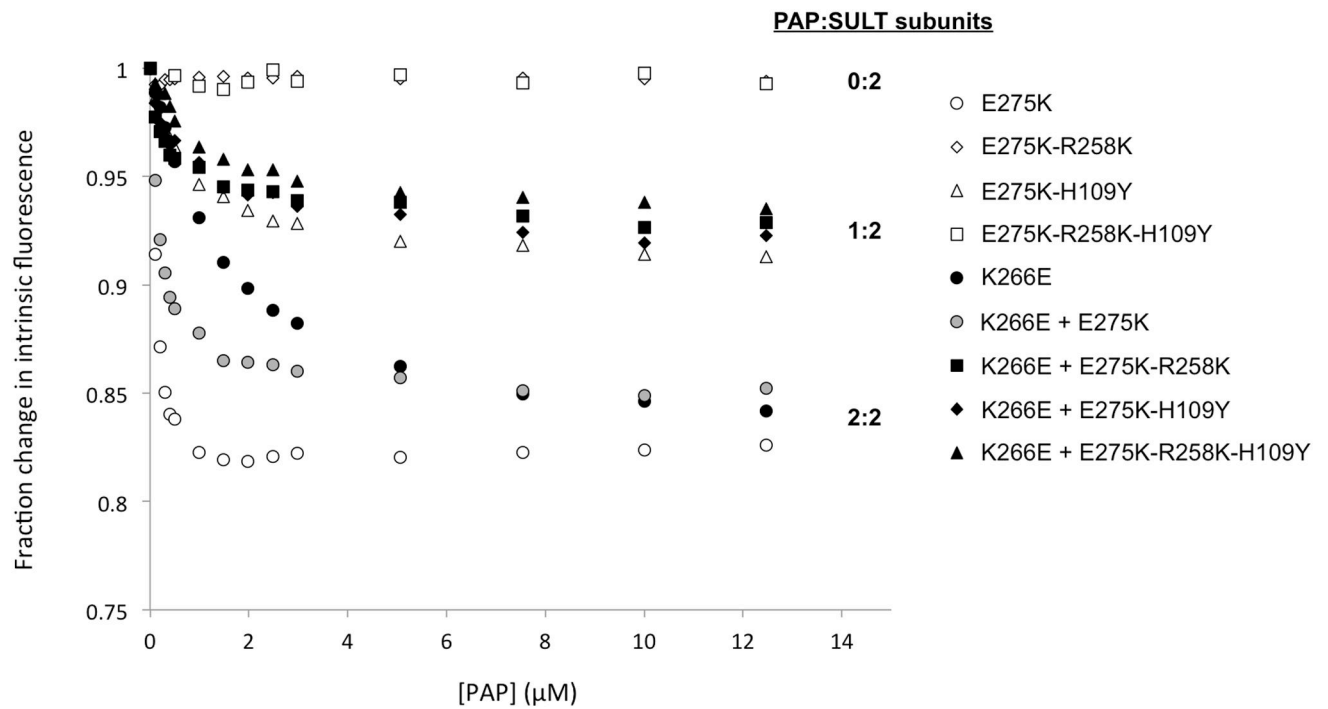


Figure 6.

Change in SULT1B1 intrinsic fluorescence (IF) upon PAP binding. Dissociation constants were derived from the IF binding curves for each E275K isoform alone and in combination with the K266E subunit (refer to key). PAP:SULT subunit stoichiometry was estimated based on the magnitude of intrinsic fluorescence change at saturation. Data are the mean values of triplicate experiments. Dissociation constant values are listed in Table 2.

SULT1B1 isoform

K266E	+	+	+	+	+					
K266E-R258K						+	+	+	+	+
K266E-H109Y										
K266E-R258K-H109Y										
E275K		+					+			
E275K-R258K			+					+		
E275K-H109Y				+					+	
E275K-R258K-H109Y					+					+

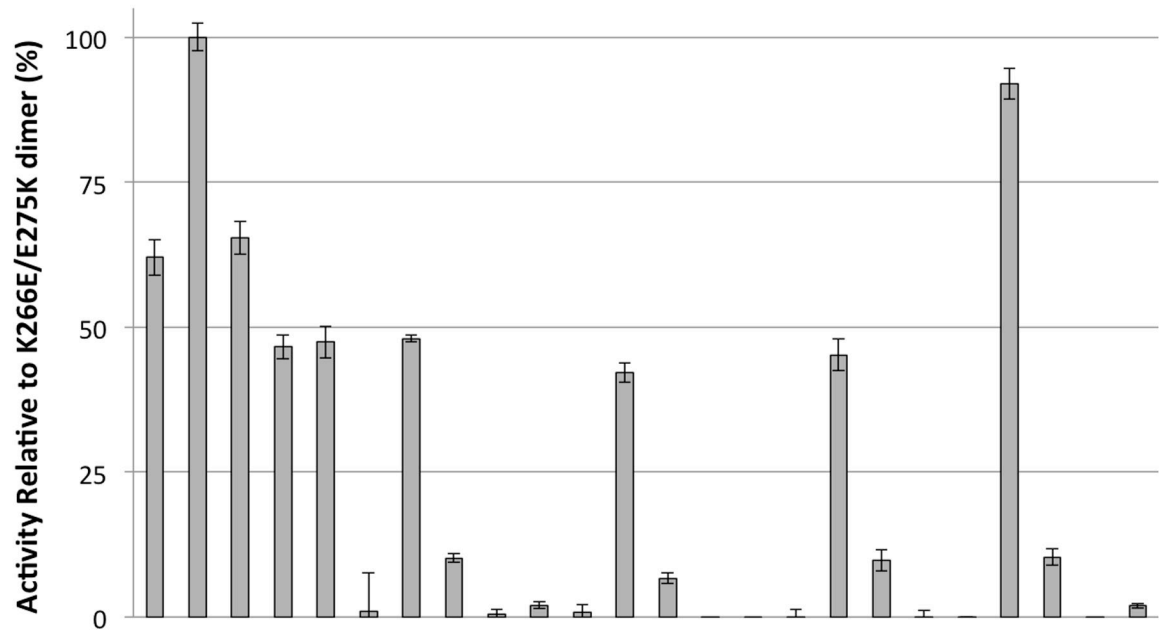


Figure 7. Specific activity of each SULT1B1 subunit by itself and after combination with each potential partnering subunit. The specific activity (normalized for protein concentration) of each isoform toward 1-naphthol is an average of three time points along the product formation curve (error bars = SEM). Each isoform is indicated by (+) signs above the graph. For ease of comparison, data were normalized to the activity of the K266E/E275K heterodimer.

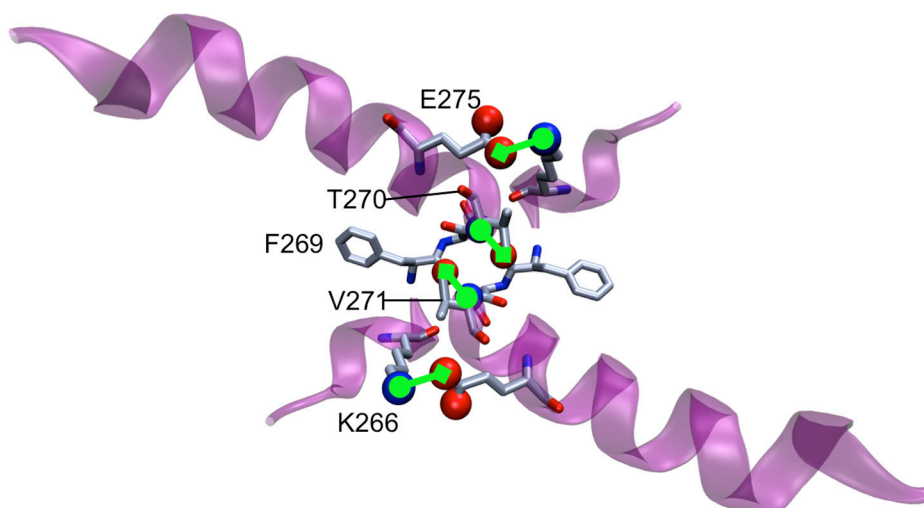


Figure 8. Key interactions along SULT dimerization interface. The non-covalent interaction (green line: box = oxygen, circle = nitrogen) between K266 and E275 is not essential for dimerization. K266 rests on a single turn helix, a secondary structure whose preservation is important for establishing the bond between the amide nitrogen of Val271 and the alpha carbon of Phe269.

Table 1

List of primers for cloning and mutagenesis.

Primer ID	Primer Sequence	Primer Purpose
1a	5' ATGCTTTCCCAAAGATATTCT	SULT1B1 sense
1b	5' GCAAGCTTGCTCATCGTTAAATCTCTGTGCGGA	SULT1B1-HindIII antisense
2a	5' TGGTGACTGGGCGAATTACTTCA	SULT1B1-K266A sense
2b	5' TGAAGTAATTCGCCAGTCACCA	SULT1B1-K266A antisense
3a	5' GCTGGTGACTGGGAGAATTAC	SULT1B1-K266E sense
3b	5' GGTGAAGTAATTCTCCAGTC	SULT1B1-K266E antisense
4a	5' GTGGCCAAAATAAGAAATTT	SULT1B1-E275K sense
4b	5' AGCATCAAATTTCTTATTTTG	SULT1B1-E275K antisense
5a	5' ATTGTGAAAACATATCTACCGACTGAT	SULT1B1-H109Y sense
5b	5' ATCAGTCGGTAGATATGTTTTCAAT	SULT1B1-H109Y antisense
6a	5' AATCCCCTTTTATGAAGAAAGGGACGGCTG	SULT1B1-R258K sense
6b	5' CAGCCGTCCTTTCTTCATAAAAGGGGATT	SULT1B1-R258K antisense

Table 2

Paired and unpaired SULT1B1 subunit dissociation constants for PAP. Potential pairing subunits are labeled “negative” or “positive” based on the net charge of their dimerization domains. The presence of both a “negative” and “positive” subunit in a single row of the table indicates a heterodimer between the two listed isoforms.

Negative Subunit	Positive Subunit	PAP K_d (μM)	
K266E	E275K	0.18 \pm	0.006
K266E	E275K-R258K	0.34 \pm	0.042
K266E	E275K-H109Y	0.59 \pm	0.065
K266E	E275K-R258K-H109Y	1.03 \pm	0.056
K266E-R258K	E275K	0.216 \pm	0.008
K266E-R258K	E275K-R258K	2.68 \pm	0.63
K266E-R258K	E275K-H109Y	2.96 \pm	0.46
K266E-R258K	E275K-R258K-H109Y	2.59 \pm	0.94
K266E-H109Y	E275K	0.23 \pm	0.02
K266E-H109Y	E275K-R258K	4.31 \pm	0.4
K266E-H109Y	E275K-H109Y	3.28 \pm	0.305
K266E-H109Y	E275K-R258K-H109Y	3.72 \pm	0.39
K266E-R258K-H109Y	E275K	0.22 \pm	0.01
K266E-R258K-H109Y	E275K-R258K	10.8 \pm	4.45
K266E-R258K-H109Y	E275K-H109Y	695.8 \pm	--
K266E-R258K-H109Y	E275K-R258K-H109Y	1.91 \pm	0.48
--	E275K	0.08 \pm	0.009
--	R258K	--	--
--	H109Y	0.668 \pm	0.031
--	R258K-H109Y	--	--
Native SULT1B1		0.106 \pm	0.009